

**Stem Cell Reports, Volume 9**

**Supplemental Information**

**Mitigating Ischemic Injury of Stem Cell-Derived Insulin-Producing Cells  
after Transplant**

**Gaetano Faleo, Holger A. Russ, Steven Wisel, Audrey V. Parent, Vinh Nguyen, Gopika G. Nair, Jonathan E. Freise, Karina E. Villanueva, Gregory L. Szot, Matthias Hebrok, and Qizhi Tang**

**Supplementary Data:**

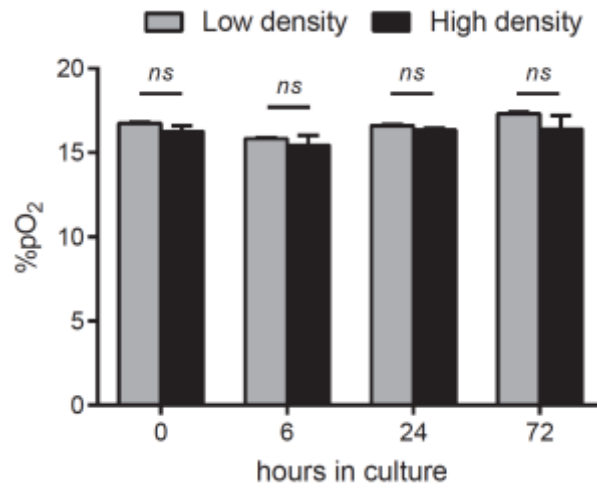


**Figure S1. Oxygen tension in low density and high density cultures.** Oxygen tensions were measured in low density and high density cultures over time. Data are expressed as mean  $\pm$  SEM and are a compilation of results from 3 independent experiments (n= 14 per condition). Statistical significance of the difference between low density and high density group was calculated using multiple t test.

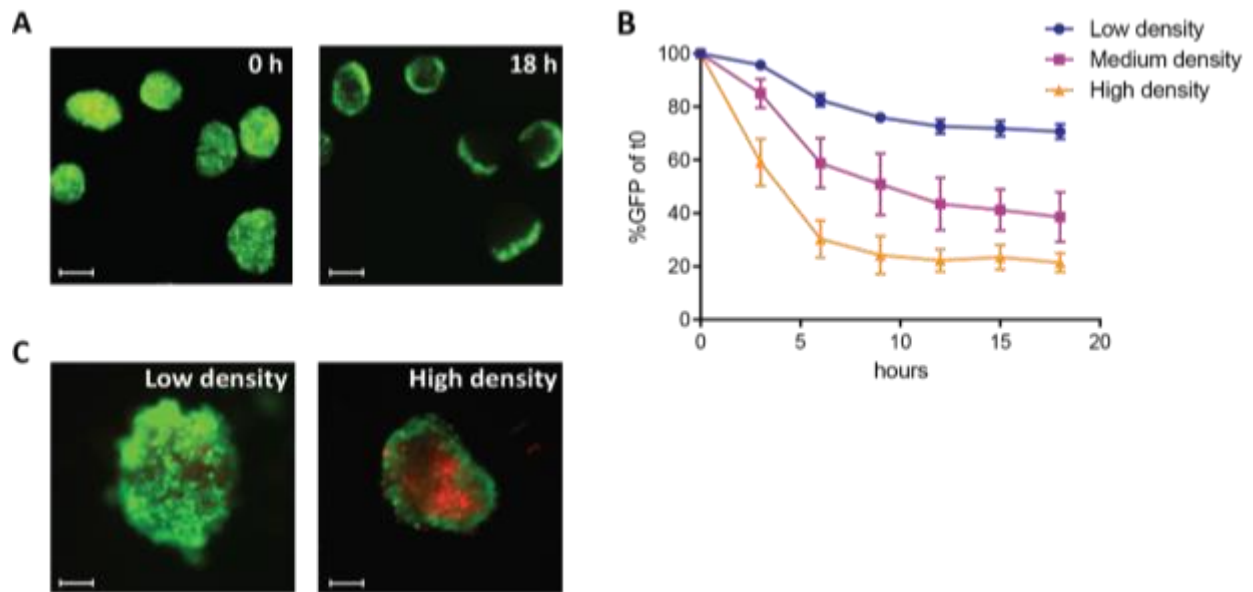


**Figure S2. Nutrient-dependent cell death *in vitro*.** (A) GFP-expressing mouse islets were cultured at high density (1000 islets/mL) and cell death resulted in loss of membrane integrity and GFP signal. Scale bar 100 $\mu$ m. (B) Kinetics of cell death of various culture densities were monitored in real time for 18 hours. Data shown as mean  $\pm$  SEM are a summary of 3 independent experiments (n=3 per condition). (C) MIP.GFP islets cultured in low- and high-density cultures stained for Propidium Iodide (red) after 6 hours. Images are representative of 3 independent experiments. Scale bar 40 $\mu$ m.

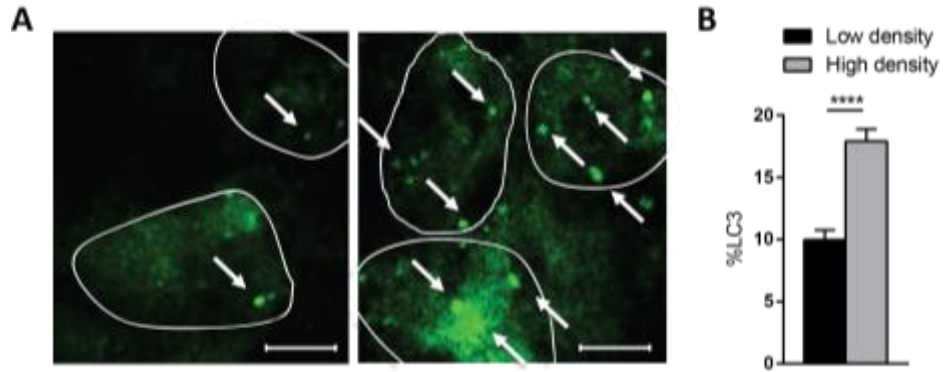


**Figure S3. Nutrient-dependent cell death in vitro.** (A) GFP-labeled LC3 autophagosome formations (arrows) in cells (outlined) in low-density (left), and high-density conditions (right) for 3 hours. Magnification 200x. Pictures shown are representative of 3 independent experiments (n=3 per group). Scale bar 5 $\mu$ m. (B) Islets are dissociated to single cells and percentage of LC3+ cells are quantified through flow cytometry (\*\*\*\*p= 0.0007). Data shown as mean  $\pm$  SEM are a summary of 3 independent experiments. Statistical significance of the difference between low-density and high-density group was calculated using paired t test.

**Table S1. Primers used for RTqPCR analysis of human SCIPC.**

Gene symbols	Forward primers	Reverse primers
<i>SLC2A1 (GLUT1)</i>	5'-GTCCCTCTCAGTGGCCATCTTT	5'-GGCCAAAGCGGTAAACGAAA
<i>SLC2A2 (GLUT2)</i>	5'-TGGAATTGACAGGACTCCCAAC	5'-TCCAGTGGAACACCCAAAACA
<i>HK1</i>	5'-AATTCTGCGGGTCAAGTGA	5'-ACTGCCGTGCACGATGTTCT
<i>HK2</i>	5'-CAAAGTGACAGTGGGTGTGG	5'-GCCAGGTCCTTCACTGTCTC
<i>GCK</i>	5'-GGAGCGTGAAGACCAAACAC	5'-GTAGTCGAAGAGCATCTCAGC
<i>PDK1</i>	5'-AGGGTTACGGGACAGATGCAG	5'-TCAGCCTCGTGGTTGGTGT
<i>LDHA</i>	5'-GCACCCAGTTTCCACCATGA	5'-TCTTCAAACGGGCCTCTTCC
<i>VEGFA</i>	5'-GCTACTGCCATCCAATCGAG	5'-ACACAGGATGGCTTGAAGATG
<i>PDX1</i>	5'-TGGAGCTGGCTGTCATGTTG	5'-GCGCTTCTTGTCCTCCTCT
<i>MCT4 (SLC16A3)</i>	5'-TCATCACTGGCTTCTCCTACGC	5'-AGCCGATCCCAAACCTCCTGT
<i>IRS1</i>	5'-CCACTCGGAAAACCTTCTTTCAT	5'-AGAGTCATCCACCTGCATCCA
<i>GADPH</i>	5'-TTGCCATCAATGACCCCTTCA	5'-CGCCCCACTTGATTTTGGA

*SLC2A1 (GLUT1)*: solute carrier family 2 (facilitated glucose transporter), member 1 (glucose transporter 1);

*SLC2A2 (GLUT2)*: solute carrier family 2 (facilitated glucose transporter), member 2 (glucose transporter 2);

*HK1*, hexokinase 1;

*HK2*, hexokinase 2;

*GCK*, glucokinase (HK4);

*PDK1*, pyruvate dehydrogenase kinase 1;

*LDHA*, lactate dehydrogenase A;

*VEGFA*, vascular endothelial growth factor A;

*PDX1*, pancreatic and duodenal homeobox 1;

*MCT4 (SLC16A3)*, monocarboxylic acid transporter 4 (solute carrier family 16, member 3);

*IRS1*, insulin receptor substrate 1;

*GADPH*, glyceraldehyde 3-phosphate dehydrogenase.

## Supplemental Experimental Procedures

### Mice

C57BL/6 (B6), B6.MIP-Luc, B6.MIP-GFP, B6.LC3-GFP, and NOD.Cg-Prkdcscid Il2rgtm1Wjl/SzJ (NSG) mice were housed and bred at the University of California, San Francisco Animal Barrier Facility. All animal procedures were performed under approved protocols and in accordance with ethical guidelines by the Institutional Animal Care and Use Committee (IACUC) at the University of California, San Francisco.

### Islet isolation

Mouse islets were isolated as previously (Szot et al., 2007). Purified islets were rested in RPMI medium overnight and healthy islets were handpicked for experiments. Human research islets provided by the UCSF DRC Islet Production Core following current standard protocols on research consented pancreas donors (Szot et al., 2009). All human studies were approved by local ethics committees. Pancreata were procured from multiorgan cadaveric donors using cold perfusion with University of Wisconsin solution (ViaSpan, DuPont Pharmaceuticals Ltd.).

### Derivation of constitutive luciferase-expressing MEL1 <sup>INS<sup>GFP/wt</sup></sup> cell line

DNA encoding a firefly luciferase gene was targeted to the AAVS1 locus of the MEL1 <sup>INS<sup>GFP/wt</sup></sup> cells using a published TALEN pair and a targeting vector containing homology sequences and a Puromycin selection (Addgene plasmid #58409, #59025, and #59026), which was modified by inserting a firefly luciferase gene via a T2A cleavage site after the Puromycin resistance gene. Human ES cells were targeted by electroporation of 5ug of each TALEN vector with 20ug of the Luciferase containing targeting vector using a Biorad GenePulser (Hercules, CA) using an exponential decay and 250V and 500uF settings. Cells were plated on DR4 resistant MEFs containing plates and selected after 24-48 hours with 0.5ug/ml Puromycin for 3-4 days. Successfully targeted cells were identified using bioluminescent followed by PCR of genomic DNA to verify site directed integration of the targeting vector. Bioluminescence imaging demonstrates a cell dose-dependent increase of bioluminescence signal (not shown).

### SCIPC differentiation

Human embryonic stem cell line containing a GFP gene knocked into the endogenous insulin locus, MEL1 <sup>INS<sup>GFP/wt</sup></sup> (Micallef et al., 2012), was maintained as described (Russ et al., 2015). Suspension-based differentiations were carried out as described previously (Russ et al., 2015) with modification of the last differentiation stages. Cultures were incubated in DMEM (Gibco) containing 25 mM glucose, 1:100 B27 (StemCell Technologies), 50 ng/ml EGF (RnD Systems), and 50 ng/ml KGF (RnD Systems) for days 9 and 10. Thereafter, clusters were incubated in DMEM (Gibco) containing 25mM Glucose supplemented with 1:100 B27 (StemCell Technologies), 1:100 non-essential amino acids (Gibco), 1mM N-Acetyl-L-Cysteine (Sigma), 10µg/ml Heparin Sodium Sulfate (Sigma), 10µM Zinc Sulfate heptahydrate (Sigma), 10µM ALK inhibitor 2 (Axxora), 2µM T3 (3,3',5-Triiodo-L-thyronine sodium salt) (Sigma), 500nM LDN-193189 (Stemgent), 1µM Gamma-Secretase inhibitor (XXi) (Millipore), 2µM Bay K 8644 (Tocris), and 0.5mM 2-Phospho-L-ascorbic acid (Sigma). Medium was changed daily by aspirating approximately 5ml followed by addition of 5ml fresh media.

### Islet metabolic measurement

Oxygen consumption rate (OCR) and extracellular acidification rate (ECAR) were quantified as previously described (Wikstrom et al., 2012). XF24 plates that are specifically designed to assess islets and similar clusters were used. 20 islets or SCIPC clusters were deposited at the bottom of individual wells and restrained by a mesh to prevent clusters dispersion. Cells were incubated for 1 hour at 37°C after which respiration was measured. Samples were analyzed using Seahorse XF24 Extracellular Flux Analyzer (Seahorse, North Billerica, MA).

### Bioluminescence Imaging

Luciferase-expressing islet or SCIPC graft mass was monitored using bioluminescence imaging as described previously (Faleo et al., 2016).

### Islet live imaging

MIP-GFP islets were used to visualize islet survival *in vitro* in real time. Isolated islets were plated into a 96-well plate at various concentration and placed on a stage of a microscope that was encased in an environmentally controlled chamber to maintain 37°C and 5% CO<sub>2</sub> throughout the experiment. Green fluorescent signal and bright field images were captured every 3 hours for an 18-hour follow-up period. The pictures were then analyzed using NIS Elements

software (Nikon) to quantify GFP signals.

### **Oxygen tension measurements**

Oxygen tensions of islet cultures were measured using the FOSPOR-PI600-2M Oxygen Sensor probe (Ocean Optics, Dunedin, FL). The probe was immersed deep into the media of each well. For each sample, 14 measurements were performed at each time point and the mean  $\pm$  SEM was calculated.

### **Flow cytometry**

To measure cell viability after *in vitro* culture, SCIPC clusters or whole islets were stained with 25 $\mu$ g/mL Propidium Iodide (PI, Sigma) for 15 minutes. The clusters were then washed in PBS 3 times before dissociation into single cells using Accumax (Innovative cell technologies, San Diego, CA). The cells were washed before analysis on an Accuri flow cytometer (BD Bioscience, San Jose, CA). To quantify cells expressing GFP after transplant, grafts were harvested from the renal capsule at day 7 and the dissociated cells were stained with PI and anti-HLA-ABC-PE-Cy5 (W6/32, A18548, Invitrogen Antibodies, Carlsbad, CA) before analysis on Accuri. Flow cytometric analyses of expression of  $\beta$  cell maturation markers by SCIPC were performed as previously described. Data were analyzed with FlowJo software (FLOWJO LLC, Ashland, Oregon).

### **GSIS assay**

GSIS was measured as described previously for islets (Kloster-Jensen et al., 2016). Insulin concentrations in supernatant were measured using enzyme-linked immunosorbent assays (ELISA) for mouse insulin (Merckodia, Uppsala, Sweden) and human C-peptide (ALPCO, Salem, NH). Stimulation index is calculated using the following formula:  $SI = \frac{[\text{Insulin}]_{\text{high glucose}}}{[\text{Insulin}]_{\text{low glucose}}}$ .

### **RTqPCR Analysis**

Total RNA was isolated from SCIPC using the RNeasy MicroKit (Qiagen, Hilden, Germany) first-strand cDNA was prepared using iScript cDNA Kit (Bio-Rad, Hercules, CA), and quantitative RT-PCR was performed on a CFX Connect Real-Time System (Bio-Rad) with FastStart Universal SYBR Green Master Mix (Roche, Basel, Switzerland). Relative changes in gene to *GADPH* ratio between hypoxic and normoxic conditions were computed using the  $2^{-\Delta\Delta C_t}$  method. See Table 1 in supplementary methods for primer sequences.

### **Immunohistochemistry**

Tissue-bearing SCIPC grafts were fixed in paraformaldehyde (Sigma), incubated overnight in 30% sucrose (Sigma), before being embedded in tissue-Tek<sup>®</sup> OCT (Sakura Finetek, Torrance, CA). A polyclonal guinea pig anti-insulin antibody (1:100, A0564, Dako, Glostrup, Denmark) was applied overnight and Alexa Fluor<sup>®</sup> 568 goat anti-guinea pig IgG (1:200, A11075, Invitrogen) was incubated for 1 hour. Images were taken using Leica SP5 upright confocal microscope (Leica Microsystems, Buffalo Grove, IL) and processed with Imaris software (Bitplane, Concord, MA).

### **Statistical Analysis**

Statistical analyses were performed with the aid of GraphPad software (GraphPad Prism, La Jolla, CA).

### **Supplemental References**

Faleo, G., Lee, K., Nguyen, V., and Tang, Q. (2016). Assessment of Immune Isolation of Allogeneic Mouse Pancreatic Progenitor Cells by a Macroencapsulation Device. *Transplantation*.

Kloster-Jensen, K., Sahraoui, A., Vethe, N.T., Korsgren, O., Bergan, S., Foss, A., and Scholz, H. (2016). Treatment with Tacrolimus and Sirolimus Reveals No Additional Adverse Effects on Human Islets In Vitro Compared to Each Drug Alone but They Are Reduced by Adding Glucocorticoids. *J Diabetes Res* 2016, 4196460.

Szot, G.L., Koudria, P., and Bluestone, J.A. (2007). Transplantation of pancreatic islets into the kidney capsule of diabetic mice. *J Vis Exp*, 404.

Szot, G.L., Lee, M.R., Tavakol, M.M., Lang, J., Dekovic, F., Kerlan, R.K., Stock, P.G., and Posselt, A.M. (2009). Successful clinical islet isolation using a GMP-manufactured collagenase and neutral protease. *Transplantation* 88, 753-756.

Wikstrom, J.D., Sereda, S.B., Stiles, L., Elorza, A., Allister, E.M., Neilson, A., Ferrick, D.A., Wheeler, M.B., and Shirihai, O.S. (2012). A novel high-throughput assay for islet respiration reveals uncoupling of rodent and human islets. *PLoS One* 7, e33023.